Accurate wavelengths of resonance lines in Zn-like heavy ions

S.B. Utter, P. Beiersdorfer, and E. Träbert

Abstract: Using an electron-beam ion trap and a flat-field spectrometer, the extreme ultraviolet resonance lines of Zn-like ions of Yb, W, Au, Pb, Th, and U were observed and their wavelengths measured with greatly improved accuracy. The results are compared to those from laser-produced plasmas and to theory, and significant differences are found.

PACS Nos.: 32.30.Jc, 39.30.+w

Résumé : On a utilisé un piège ionique à faisceaux électroniques pour la production des spectres résonants UVE dans des ions isoélectroniques du Zn, les éléments Yb, W, Au, Th et U et avons mesuré les longueurs d'ondes avec une précision grandement améliorée. Les mesures sont comparées avec des résultats obtenus dans des plasmas générés par laser et avec des calculs. On a trouvé des différences significatives.

[Traduit par la Rédaction]

1. Introduction

One- and two-valence electron ions are being studied along extended sections of the isoelectronic sequences, because their ground-state transitions stand out from many spectra. Consequently, they can be accurately measured and be compared to the results of highly developed calculations, providing important benchmarks through both precision experiments and modern atomic structure theory. In a companion study [1], we have presented data on Cu-like ions, recorded as extreme ultraviolet (EUV) spectra at an electron-beam ion trap (EBIT). Elaborate calculations of the transition energies in the Cu isoelectronic sequence agree well with each other. The experimental data from very powerful lasers like NOVA and OMEGA [2–5], however, show a systematic deviation from the predicted trend for high-nuclear charge Z. In contrast to that, measurements under low-density conditions, using an electron-beam ion trap, corroborate the calculations, except for the very highest values of Z [1].

In the following we extend our study of highly charged ions in the Cu isoelectronic sequence to the Zn isoelectronic sequence. Here, an additional electron in the valence shell adds some complexity to the calculation (two electrons are in the same valence shell). From an experimental point of view, however, the $4s^2\,{}^1S_0 - 4s4p\,{}^1P^o_1$ transition in the Zn-like ion is close in wavelength to the $4s\,{}^2S_{1/2} - 4p\,{}^2P^o_{3/2}$ transition in the Cu-like ion. Therefore, the same recordings made for the study of Cu-like ions yield a second set of almost equally precise data on Zn-like ions. Our measurements cover the six

Received 24 December 2002. Accepted 31 March 2003. Published on the NRC Research Press Web site at http://cjp.nrc.ca/ on 28 August 2003.

S.B. Utter,[1] P. Beiersdorfer,[2] and E. Träbert. Division of Physics and Advanced Technologies, Lawrence Livermore National Laboratory, Livermore, CA 94550-9234, U.S.A.

[1]Present address: Spectra-Physics, Mountain View, CA 94039, U.S.A.
[2]Corresponding author (e-mail: beiersdorfer@llnl.gov).

 doi: 10.1139/P03-071

elements Yb ($Z = 70$), W ($Z = 74$), Au ($Z = 79$), Pb ($Z = 82$), Th ($Z = 90$), and U ($Z = 92$). All previous measurements of high-Z ($Z \geq 70$) elements were made using laser-produced plasmas [1–5]. The present measurements are the first from a low-density source, extending measurements of mid-Z elements made at tokamaks [6–8]. The tokamak measurements have agreed well with theoretical predictions, and it would be valuable to see whether low-density measurements of the highest Z Zn-like ions also agree better with theory than with laser measurements, similar to what was found for the Cu isoelectronic sequence. If some of the difficulties with the laser plasma data on Cu-like ions were the result of satellite-line contamination, the situation might be different for the Zn-like ions. The new data on Zn-like ions are then compared with separate calculational results, recognizing the much larger difficulties encountered with a second electron in the valence shell.

2. Experiment

The experiment was done at the University of California Lawrence Livermore National Laboratory EBIT-II electron-beam ion trap [9, 10]. Ions of the respective species were introduced into EBIT-II by means of a metal vapour vacuum arc ion source (MeVVA). Ions were trapped by the combination of a strong (3 T) magnetic field for radial confinement, electric fields in a drift tube arrangement for axial confinement, and the attractive potential and space charge compensation provided by the electron beam. The ions were bombarded by the same electron beam, so that they were ionized in a stepwise fashion until reaching a charge state that had an ionization energy higher than the collision energy available from the kinetic energy of the electron beam. The energy necessary to create Cu-like ions is of the order 2–4.5 keV for the elements considered here.[3] The next ionization step, opening the $3d^{10}$ shell (that is, exciting Ni-like ions), requires much more energy. Therefore, a wide range of electron beam energies was suitable to create a charge state balance that favoured Cu- and Ni-like ions by burning out the lower charge states. The resulting EUV spectra are very "clean" and show mostly lines from Cu-like and Zn-like ions when optimized for the production of the former. Optimization for the latter ions would bring up lines from lower charged ions (in particular the spectra of Ga- and Ge-like ions), which would contaminate the profiles of the lines of present interest [1, 11].

The present measurements employed a flat-field spectrometer (FFS) [12] with a 2400 ℓ/mm variable line-spaced concave grating [13] and equipped with a cryogenically cooled back-thinned CCD camera. The camera chip has 1024×1024 pixels on an area of about 25 mm squared. The FFS imaged the light from the 50 μm wide excitation zone in the ion trap, without any entrance slit, onto the CCD chip where it resulted in the geometrically expected width of about 2 pixels [10].

Due to minor spectral aberrations, the image of each line is slightly curved at the CCD surface. Simple summing across the dispersion direction would, therefore, broaden the spectral line recordings. Instead, each file was binned into one, three, or eight columns depending on the line intensity. Each of the sections was independently calibrated, effectively increasing the number of only loosely dependent results. Calibration referred to a number of well-known transitions in H- and He-like ions of C, N, and O, in Li-like ions of Ne, and in Ne-like ions of Ar, fitting a third-order polynomial to the reference line positions. (For reference line wavelengths, see the on-line data bases [14, 15] and the references therein.)

Each two-dimensional CCD image was filtered for cosmic-ray events. The background light emission recorded by the CCD was determined by running EBIT-II with an "inverted" trap [16], that is, with the middle drift tube at a higher potential than the top drift tube, so that no trapping occurred and any ions would be expelled, and with no neutral gas being injected. Since there is some random noise associated with the readout of each CCD image, several background spectra were averaged and smoothed before they were subtracted from the data files. We present our experimental results on Zn-sequence ions in

[3] J.H. Scofield. Calculated data. Private communication.

Fig. 1. Spectra of Yb, Pb, and Th with the prominent lines arising from Cu-like and Zn-like ions, respectively. In the Yb spectrum, the nearby lines from ions of lower charge states are both weak (from optimizing the charge state balance) and well-resolved from the lines of interest. The appearance of C lines in the Pb spectrum occur because of the particular material (mostly graphite) used in that particular MeVVA ion source. With Th, the charge state balance was less favourable than for the other elements (see text), leading to a contamination of the line from the Zn-like ion by emission from lower charge states. This, of course, results in a larger wavelength uncertainty, despite the favourable calibration situation.

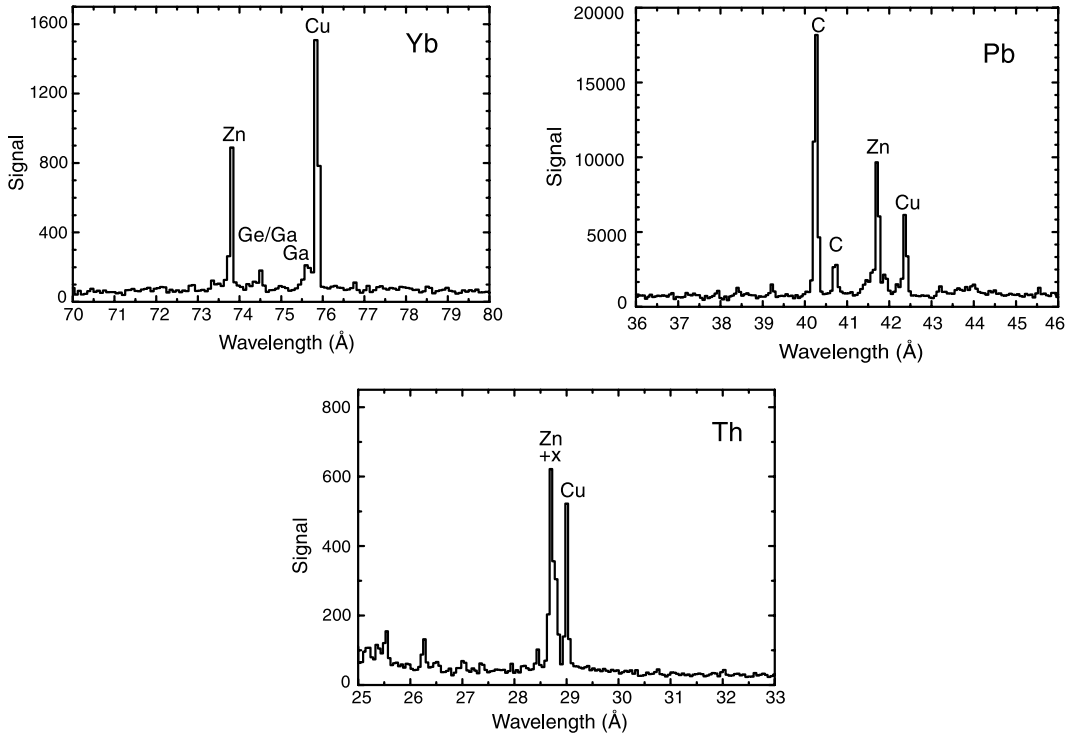

Table 1. A description of the measurements is given in the following sections. Because details of the ion production, observation, evaluation, and calibration techniques have been presented elsewhere [1], only a few specific explanations will be given here.

2.1. Ytterbium

With a wavelength of near 75 Å, the resonance transition in the Zn-like ion of Yb fits well into the optimal working range of the 2400 ℓ/mm grating. Nitrogen, carbon, and neon transitions were used for the calibration of the entire spectral range. Carbon is regularly found in background spectra as a contaminant, N_2 gas can easily be injected if needed. Eleven well-known transitions in hydrogen-like and helium-like ions of carbon and nitrogen in the range 25–40 Å, and of lithium-like neon ions in the range 56–88 Å were used to calibrate the detector over the entire spectral range of 23.4–90.8 Å. The precision of this measurement was limited by the lack of precise calibration lines near the long-wavelength end of the spectrum. Specifically, the Li-like Ne transitions used in the calibration have a wavelength uncertainty of 5 mÅ, which added an uncertainty of about 3 mÅ to the calibration in the 75 Å region of the spectrum.

The Yb spectra were recorded at an electron-beam energy of $E_{\mathrm{beam}} = 2.51$ keV. Each spectrum (Fig. 1) resulted from an integration of 20 min of observation. Observation for 9 h (plus recordings for background and calibration) resulted in 27 measurements of this transition. By varying the energy of the electron beam above and below the threshold to produce the Cu-like charge state, the $4s_{1/2} - 4p_{3/2}$

Table 1. Predicted and measured wavelengths of the $4s^2\,{}^1S_0$ – $4s4p\,{}^1P^o_1$ transition in Zn-like ions. All wavelength values are given in Å.

Element	Z	Theory	Experiment [i]	Experiment *
Yb	70	73.430[a]	73.792(20)	73.8070(66)
		73.8[b]		
		73.368[c]		
		73.784[d]		
W	74	60.629[a]	60.900(20)	60.9300(54)
		61.0[b]		
		60.585[c]		
		60.907[d]		
		60.515[e]		
		60.806[f]		
		60.59[g]		
		61.08[h]		
Au	79	48.0[b]	48.063(20)	48.0583(49)
		47.787[c]		
		48.038[d]		
		47.7[e]		
		47.991[f]		
		47.97[g]		
		48.27[h]		
Pb	82	41.7[b]	41.689(20)	41.7185(45)
		41.483[c]		
		41.708[d]		
		41.681[f]		
		41.73[g]		
		41.95[h]		
Th	90	28.6[b]	28.702(20)	28.7227(67)
		28.52[c]		
		28.704[d]		
		28.707[f]		
U	92	26.1[b]	26.157(20)	26.1868(36)
		25.975[c]		
		26.152[d]		
		25.8[e]		
		26.168[f]		
		26.32[g]		
		26.40[h]		

[a] Multiconfiguration Dirac–Fock (MCDF) [23].
[b] Semiempirical analysis of experimental data [24].
[c] HULLAC [5].
[d] HULLAC plus semiempirical correction [5].
[e] Relativistic random-phase approximation (RRPA) [21].
[f] Multiconfiguration Dirac–Fock (MCDF), with QED, including nuclear size effects [22].
[g] Multiconfiguration Dirac–Fock (MCDF), with QED [25].
[h] Multiconfiguration relativistic random-phase approximation (MCRRPA), with QED [25].
[i] Ref. 5.
* This work.

transition in the Cu-like ions and the $4s^2\,{}^1S_0 - 4s4p\,{}^1P_1^o$ transition in the Zn-like ion were easily recognized. These two, as well as two significantly weaker lines, were fit in all 27 sections. Each of these lines was well resolved from the others.

2.2. Tungsten

The electron-beam energy was varied systematically from 1.7 to 3.0 keV, that is, both well above and below threshold for the production of the Cu-like ion [11]. All spectra with significant intensity from the Cu-like ion were also used to obtain information on the Zn-like ion.

2.3. Gold

The Au data were recorded at the optimal energy for the production of the Cu-like charge state ($E_{\text{beam}} = 4.01$ keV). For this measurement the flat-field spectrometer was arranged to cover the wavelength range 14.6–73.0 Å. The wavelengths of the transitions of interest in the Cu- and Zn-like ions of Au, near 48–49 Å, are in a gap between the calibration lines available from C and Ne. However, two transitions in Ne-like Ar, with wavelengths of 48.730 and 49.180 Å, respectively [17], or 48.737 and 49.181 Å, respectively [18], were found to be very near by and augmented the others.

Lower precision data on Cu- and Zn-like Au ions have been reported from an independent survey of Au spectra using the same electron-beam ion trap and detection system, but less elaborate calibration procedures [19]. That work supports the spectral analysis presented here.

2.4. Lead

For Pb, the line of interest in the Zn-like ion is near the carbon absorption edge that affects the measurement because of a slight oil contamination of the CCD chip surface. This suppresses the signal intensity. Nevertheless, the line of interest in the Zn-like ion was seen well above the noise level and somewhat stronger than that from the Cu-like ion (Fig. 1). Besides the line of primary interest, the spectrum shows two lines of He-like C (the decays of the $1s2p\,{}^1P_1^o$ and ${}^3P_2^o$ levels, respectively). This reflects the particular material used in this MeVVA, a mixture dominated by graphite, with only a small admixture of Pb.

2.5. Thorium

The precision of the thorium measurements benefits from the wavelength (near 28.7 Å) being close to the resonance and intercombination lines in the He-like ion of N (at 28.7870 and 29.0843 Å [20]). However, the width of the line indicates a blend with a line (or lines) from lower ionization stages, as indicated in the sample spectrum shown in Fig. 1. This blending has considerably increased our error limit.

2.6. Uranium

The wavelength of the Zn-like U transition is near 26.2 Å. Therefore, the lines of N and O were ideal for calibration. Three sets of U data were accumulated. Two of the sets were obtained at $E_{\text{beam}} = 6.79$ keV, whereas the third was at a higher energy, $E_{\text{beam}} = 8.10$ keV. At the higher energy, above the ionization potential of the Ni-like charge state ion, the data accumulation rate from the Zn-like charge state was significantly lower.

3. Results and discussion

To estimate the reliability and reproducibility of the measurements, a variety of tests was performed. Besides repeated measurements, often under varied conditions, parallel strips of the spectral images on the detector were calibrated and analyzed separately. The scatter of the individual results as well as the

Fig. 2. Theoretical (ab initio and semiempirically corrected) wavelength data on Zn-like ions in the high-Z range. All values have been normalized to the results of calculations by Brown et al. [5] using the HULLAC code. This reference was chosen, because it was the only one available for all elements covered by our measurements and not tainted by semiempirical corrections. The data set labels (in chronological order) are the same as in Table 1. Theory: (a) Biémont, MCDF [23], (b) Curtis, semiempirical analysis [24], (c) Brown et al. HULLAC [5], (d) Brown et al. HULLAC plus semiempirical corrections [5], (e) Shorer and Dalgarno, RRPA [21], (f) Cheng and Wagner, MCDF [22], (g) Cheng and Huang, MCDF [25], and (h) Cheng and Huang, MCRRPA [25].

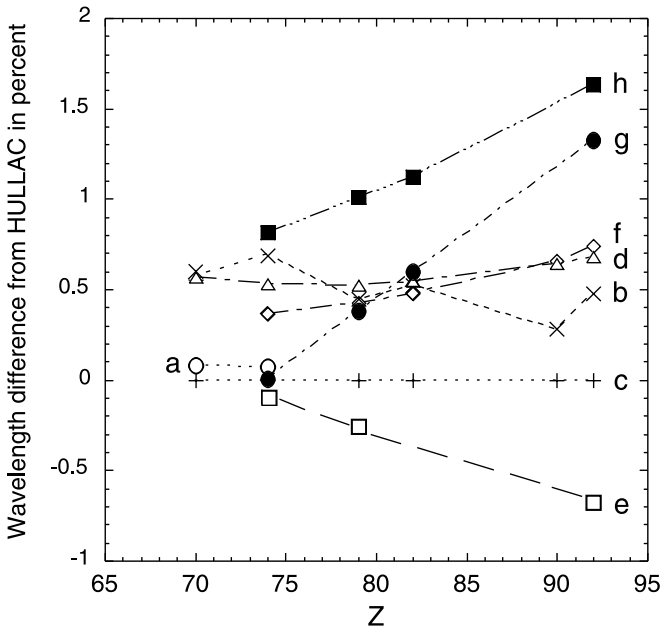

statistical significance of the line position values lead us to a statistical uncertainty ($1\,\sigma$). The precisely calculated or measured transitions in hydrogen- or helium-like ions that were used for calibration are known to better than 0.001 Å, but, conservatively, a systematic error of 1 mÅ has been assigned to each measured line. Beyond 45 Å, it became necessary to use transitions from the Li and Ne isoelectronic sequences with their less well-known wavelengths, increasing the associated systematic error. The statistical and systematic error estimates were added in quadrature to yield the combined error estimates that are listed alongside our wavelength results in Table 1. Wherever it was possible to measure a well-known independent transition, agreement with the known wavelength values was much better than these error ranges.

In Table 1, we select from the available experimental data [2–5] only the latest set of measurements. In comparison to that, our wavelength data represent an improvement by a factor of three to five. For $Z < 80$, the new data are compatible with the older ones within the mutual errors. This is different from the results for the $4s_{1/2} - 4p_{3/2}$ transition in Cu-like ions, where our low-density results differed markedly from the laser plasma results. Our results lie apart from those [5] for $Z \geq 82$ (Pb). A slight offset among the experimental values for Th expands to a slight discrepancy (outside the mutual $1-\sigma$ estimates) in U, similar to our findings on the Cu isoelectronic sequence [1].

Figure 2 displays the results of different calculations [5, 21–25]. Figure 3 compares two of the calculations with the measured data. Evidently, the situation is far from clear. The various calculations feature different isoelectronic trends, with slopes (relative to the experimental trend) pointing up or down. Calculations that seem to come close to the experimental data mostly involve semiempirical adjustments (by 0.5% in case of the HULLAC calculations performed by Brown et al. [5]) guided by the earlier (lower Z) experimental data. We, therefore, refer all results to the HULLAC results before

Fig. 3. Experimental and theoretical wavelengths on Zn-like ions in the high-Z range. The scaling is the same as in Fig. 2, referring to the HULLAC code results obtained by Brown et al. [5]. Only one of the theoretical predictions (f) [22]) is shown and thus the scale could be expanded. Experiment: (A) Brown et al. [5], (B) This work.

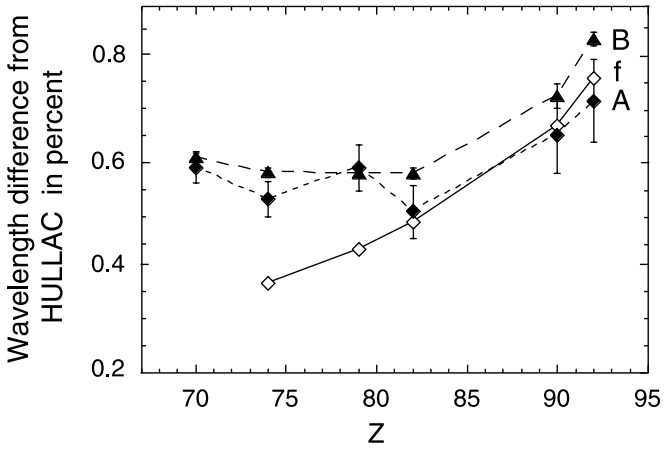

adding the correction. Interestingly, our data show a smooth trend with the nuclear charge, clearly smoother (and perhaps more internally consistent) than the trend of the experimental data presented by Brown et al. [5]. Up to about $Z = 82$, the deviation between this trend and the HULLAC result is described by a fixed percentage error of the calculation. At the highest nuclear charges, the deviation widens.

For Th and U, our data agree best with the predictions by Cheng and Wagner [22], but for Pb and lighter elements there is a notable discrepancy (Fig. 3). Cheng and Wagner claim good agreement with the earlier experimental results obtained by Seely et al. [2]. If their lower Z predictions were shifted to match our experimental data up to, say, $Z = 79$ (Au), a discrepancy would appear with the highest Z data. The mismatch there would be comparable to that noted between predictions and measurements for the highest Z ions in the Cu isoelectronic sequence [1]. Next in proximity to the present experimental data are the semiempirically corrected results of the HULLAC code calculations by Brown et al. [5] and of a semiempirical analysis by Curtis [24]. Alas, such semiempirically corrected calculations have a very limited predictive power. All other calculations depicted do worse.

In any case, none of the calculations on the Zn sequence apparently is as good as the best available on the Cu sequence (see ref. 1). Much better calculations for the Zn sequence ions are needed to demonstrate a correspondingly high level of understanding of the atomic structure as has been reached for Cu-like ions. Such calculations seem possible now, since corresponding improvements have been achieved very recently on Na- to Si-like ions [26].

Acknowledgement

We are happy to acknowledge the dedicated technical support of Ed Magee and Phil D'Antonio. The work at the University of California Lawrence Livermore National Laboratory was performed under the auspices of the Department of Energy under Contract No. W-7405-Eng-48.

References

1. S.B. Utter, P. Beiersdorfer, E. Träbert, and E.J. Clothiaux. Phys. Rev. A: At. Mol. Opt. Phys. **67**, 032502 (2003).
2. J.F. Seely, J.O. Ekberg, C.M. Brown, U. Feldman, W.E. Behring, J. Reader, and M.C. Richardson. Phys. Rev. Lett. **57**, 2924 (1986).
3. J.F. Seely, C.M. Brown, and W.E. Behring. J. Opt. Soc. Am. B, **6**, 3 (1989).

4. N. Acquista and J. Reader. J. Opt. Soc. Am. B, **1**, 649 (1984).
5. C.M. Brown, J.F. Seely, D.R. Kania, B.A. Hammel, C.A. Back, R.W. Lee, and A. Bar-Shalom. At. Data Nucl. Data Tables, **58**, 203 (1994).
6. E. Hinnov, P. Beiersdorfer, R. Bell, J. Stevens, S. Suckewer, S. von Goeler, A. Wouters, D. Dietrich, M. Gerassimenko, and E. Silver. Phys. Rev. A: Gen. Phys. **35**, 4876 (1987).
7. P. Beiersdorfer, S. von Goeler, M. Bitter et al. Phys. Rev. A: Gen. Phys. **37**, 4153 (1988).
8. S. von Goeler, P. Beiersdorfer, M. Bitter et al. J. Phys. (Paris), **49**, C181 (1988).
9. M.A. Levine, R.E. Marrs, J.R. Henderson, D.A. Knapp, and M.B. Schneider. Phys. Scr. T, **22**, 157 (1988).
10. M.A. Levine, R.E. Marrs, J.N. Bardsley et al. Nucl. Instrum. Methods B, **43**, 431 (1989).
11. S.B. Utter, P. Beiersdorfer, and E. Träbert. Can. J. Phys. **80**, 1503 (2002).
12. S.B. Utter, G.V. Brown, P. Beiersdorfer, E.J. Clothiaux, and N.K. Podder. Rev. Sci. Instrum. **70**, 284 (1999).
13. T. Harada and T. Kita. Appl. Opt. **19**, 3987 (1980).
14. R.L. Kelly. On-line data base at `http://cfa-www.harvard.edu/amdata/ampdata/kelly/kelly.html`
15. On-line data base at `http://www.physics.nist.gov/cgi-bin/AtData/main_asd`
16. S.B. Utter, P. Beiersdorfer, and G.V. Brown. Phys. Rev. A: At. Mol. Opt. Phys. **61**, 030503 (2000).
17. L.W. Phillips and W.L. Parker. Phys. Rev. **60**, 301 (1941).
18. J.K. Lepson, P. Beiersdorfer, E. Behar, and S.M. Kahn. Astrophys. J. **590**, 604 (2003).
19. E. Träbert, P. Beiersdorfer, K.B. Fournier, S.B. Utter, and K.L. Wong. Can. J. Phys. **79**, 153 (2001).
20. G.W.F. Drake. Can. J. Phys. **66**, 586 (1988).
21. P. Shorer and A. Dalgarno. Phys. Rev. A: Gen. Phys. **16**, 1502 (1977).
22. K.T. Cheng and R.A. Wagner. Phys. Rev. A: Gen. Phys. **36**, 5435 (1987).
23. E. Biémont. At. Data Nucl. Data Tables, **43**, 163 (1989).
24. L.J. Curtis. J. Opt. Soc. Am. B, **9**, 5 (1992).
25. T.-C. Cheng and K.-N. Huang. Phys. Rev. A, **45**, 4367 (1992).
26. P. Beiersdorfer, M.H. Chen, K.-T. Cheng, and J. Sapirstein. DAMOP 2002 — Williamsburg, Va. U.S.A. May 2002.